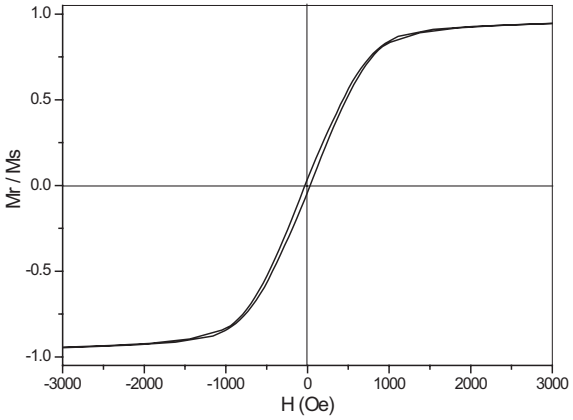

Fig. 4. Hysteresis loop of the hollow Ni submicrometer-sized spheres, at room temperature.

the reaction system have a significant influence on the formation of hollow Ni spheres. The shape of the original template was imprinted after the reaction. It is expected that this emulsion system can be extended to the synthesis of other hollow metal spheres. Such hollow metal spheres have a variety of promising applications, for example: as catalysts; as magnetic and gas storage materials; and as low-density materials. Currently, the preparation and properties of Ni and other hollow metal spheres are underway in our laboratories.

Experimental

Materials: Nickel sulfate, boric acid, ammonium fluoride, sodium hypophosphite monohydrate, cyclohexane, and polyglycol (M_w 20 000) were of commercial grade and were used without further purification.

Preparation of the Hollow Ni Submicrometer-Size Spheres: In a typical experiment, 2.5 g of polyglycol was first dissolved in 20 mL of deionized water, and then 47 mg (67.5 mM) NH_4F, 246 mg (200 mM) H_3BO_3, 112 mg (20.0 mM) $NiSO_4$, and 212 mg (100 mM) $NaH_2PO_2{\cdot}H_2O$ were added to the solution. After that, 0.5 mL of cyclohexane was injected into 5 mL of the above solution. This mixture first was treated under ultrasonic radiation for 30 min at 20 °C to make an emulsion system, and then at 75 °C to induce the reducing reaction. After a period of time, the mixture foamed and the color of the mixture turned from green to light black, meaning that nickel was formed. The color of the mixture gradually turned blacker. 5 or 10 min after the mixture turned from green to light black, the mixture was cooled to room temperature. Finally, the mixture was separated by centrifugation. The deposit was collected, washed with deionized water several times, and dried in air: black, hollow nickel spheres were obtained.

Structural characterization was performed by means of X-ray diffraction using a D/Max-RA diffractometer with Cu Kα radiation, TEM (JEM-200CX TEM) working at an accelerating voltage of 100 kV, and SEM operating at an accelerating voltage of 20 kV. EDS was performed on the microscope with a PV9100 scanning electron microanalyzer. Room-temperature magnetic characterization of the hollow Ni spheres was performed by using a Lake Shore 7303-9309 vibrating sample magnetometer (VSM).

Received: April 24, 2003
Final version: July 22, 2003

[1] a) F. Caruso, *Chem. Eur. J.* **2000**, *6*, 413. b) D. L. Wilcox, M. Berg, T. Bernat, D. Kellerman, J. K. Cochran, *Hollow and Solid Spheres and Microspheres: Science and Technology Associated with Their Fabrication and Application*, Materials Research Society Proceedings, MRS, Pittsburgh, PA **1995**, p 372. c) C. E. Fowler, D. Khushalani, S. Mann, *J. Mater. Chem.* **2001**, *11*, 1968.

[2] a) P. Tartaj, T. González-Carreño, C. J. Serna, *Adv. Mater.* **2001**, *13*, 1620. b) M. R. Al-Ubaidi, J. Anno, *Fusion Technol.* **1989**, *16*, 464.

[3] a) F. Caruso, R. A. Caruso, H. Möhward, *Science* **1998**, *282*, 1111. b) L. Wang, T. Sasaki, Y. Ebina, K. Kurashima, M. Watanabe, *Chem. Mater.* **2002**, *14*, 4827. c) F. Caruso, X. Shi, R. A. Caruso, A. Susha, *Adv. Mater.* **2001**, *13*, 740. d) I. L. Radtchenko, G. B. Sukhorukov, N. Gaponik, A. Kornowski, A. L. Rogach, *Adv. Mater.* **2001**, *13*, 1684.

[4] P. V. Braun, S. I. Stupp, *Mater. Res. Bull.* **1999**, *34*, 463.

[5] a) D. H. W. Hubert, M. Jung, A. L. German, *Adv. Mater.* **2000**, *12*, 1291. b) H. T. Schmidt, A. E. Ostafin, *Adv. Mater.* **2002**, *14*, 532.

[6] T. Liu, Y. Xie, B. Chu, *Langmuir* **2000**, *16*, 9015.

[7] a) D. Walsh, B. Lebeau, S. Mann, *Adv. Mater.* **1999**, *11*, 324. b) P. J. Brusinsma, A. Y. Kim, J. Liu, S. Baskaran, *Chem. Mater.* **1997**, *9*, 2507. c) M. Jafeliccit, Jr., M. R. Davalos, F. Jose de Santos, A. Jose de Santos, *J. Non-Cryst. Solids* **1999**, *247*, 98.

[8] D. Wang, F. Caruso, *Chem. Mater.* **2002**, *14*, 1909.

[9] J. Huang, Y. Xie, B. Li, Y. Liu, Y. Qian, S. Zhang, *Adv. Mater.* **2000**, *12*, 808.

[10] a) T. G. Wang, D. D. Elleman, J. M. Kendall, Jr., *US Patent 4 449 901*, **1984**. b) R. A. Frosch, T. G. Wang, D. D. Elleman, *US Patent 4 279 632*, **1981**.

[11] J. K. Cocharn, Jr., *US Patent 4 867 931*, **1989**.

[12] M. Jaeckel, H. Smiguski, *US Patent 4 917 857*, **1990**.

[13] a) S. Kim, M. Kim, W. Y. Lee, T. Hyeon, *J. Am. Chem. Soc.* **2002**, *124*, 7642. b) D. Zhang, L. Qi, J. Ma, H. Cheng, *Adv. Mater.* **2002**, *14*, 1499. c) S. Chah, J. H. Fendler, J. Yi, *J. Colloid Interface Sci.* **2002**, *250*, 142. d) Y. Sun, B. Mayers, Y. Xia, *Adv. Mater.* **2003**, *15*, 641.

[14] Q. Yang, K. Tang, C. Wang, Y. Qian, S. Zhang, *J. Phys. Chem. B* **2002**, *106*, 9227.

[15] a) L. Qi, H. Cölfen, M. Antonietti, *Angew. Chem. Int. Ed.* **2000**, *39*, 604. b) H. Cölfen, L. Qi, *Chem. Eur. J.* **2001**, *7*, 106.

[16] *X-ray Diffraction Procedures for Polycrystalline and Amorphous Materials* (Eds: H. P. Klug, L. E. Alexander), Wiley, New York **1962**, p. 491.

[17] *The Fundamentals and Practice of Electroless Plating* (Eds: X. Jiang, W. Shen), National Defence Industry Press, Beijing, China **2000**, p. 57.

[18] S. Chikazumi, *Physics of Magnetism*, John Wiley & Sons, New York **1964**.

Large-Area Nanowire Arrays of Molybdenum and Molybdenum Oxides: Synthesis and Field Emission Properties**

By *Jun Zhou*, *Ning-Sheng Xu*,* *Shao-Zhi Deng*, *Jun Chen*, *Jun-Cong She*, and *Zhong-Lin Wang*

There is growing interest in nanowires of metals and related oxides because of their potential applications in nanoscale electronic and optoelectronic devices.[1,2] The template-based method is one of the techniques used for synthesizing nanowires.[3–7] However, for large-area electronic applications, such as field-emission displays, new synthetic methods may

[*] Prof. N.-S. Xu, J. Zhou, Prof. S.-Z. Deng, Prof. J. Chen, J.-C. She
State Key Lab of Optoelectronic Materials and Technologies
and
Gungdong Province Key Laboratory of Display Materials and Technologies
SunYat-Sen (Zhongshan) University
Guangzhou, 510 275 (P.R. China)
E-mail: stsxns@zsu.edu.cn
Prof. Z.-L. Wang
School of Materials Science and Engineering
Georgia Institute of Technology
Atlanta, GA 30332-0245 (USA)

[**] N.-S. Xu, S.-Z. Deng, and Jun Chen thank the National Natural Science Foundation of China, the Ministry of Science and Technology of China, the Education Ministry of China, the Department of Education and Department of Science and Technology of Guangdong Province, and the Department of Science and Technology of Guangzhou City for their financial support of this project.

 DOI: 10.1002/adma.200305528

ADVANCED MATERIALS

need to be developed. Thermal evaporation, a very mature technique for thin-film deposition, is particularly useful for large-area thin film preparation, and is relatively simple, straightforward, and cost-effective.

Molybdenum is an important refractory metal: It has a very high melting point and high electrical conductivity and toughness.[8–10] Its oxides mainly include MoO_2 and MoO_3, which have many advanced applications as catalysts, sensors, photochromic and electrochromic materials, and recording materials.[11–14] Despite their importance, success in growing nanowires of Mo and its oxides is rare. Zach et al.[15] formed molybdenum oxide (MoO_x) nanowires on a stepped graphite surface by an electrochemical method, and obtained metallic molybdenum nanowires by further reduction in hydrogen. The nanowires were parallel to the substrate surface. Li et al.[16] have synthesized MoO_3 nanobelts by a solution method. Here, we report a novel procedure developed for growing well-aligned nanowire arrays of Mo and its oxides vertically oriented on the substrates and covering a large area. Molybdenum dioxide nanowire arrays were first synthesized by thermal evaporation in a vacuum chamber. With further treatment in the growth chamber, the above nanowire arrays could be turned into molybdenum trioxide nanowire arrays or metallic molybdenum nanowire arrays. The field emission properties of these nanowires have been fully investigated.

MoO_2 nanowire arrays were first grown on silicon substrates by heating a Mo boat to ~1100 °C under a constant flow of argon for 60 min in a vacuum chamber. The surface of the substrates appeared dark after the reaction. When the as-synthesized MoO_2 nanowire arrays were treated at 400 °C for 30 min in a flow of argon mixed with oxygen, they completely transformed into MoO_3 nanowires. On the other hand, they could be completely changed to metallic Mo nanowire arrays by heating the MoO_2 nanowire arrays at 800 °C for 10 h in the vacuum chamber in a flow of hydrogen gas.

Figure 1a shows the X-ray diffraction (XRD) spectrum recorded from the as-formed MoO_2 nanowires. The MoO_2 nanowires have a monoclinic structure, with lattice parameters: $a = 5.61$ Å, $b = 4.86$ Å, $c = 5.54$ Å, and $\theta = 119.37°$ (Joint Committee on Powder Diffraction Standards, JCPDS: 32-671). Peaks of Mo of body-centered cubic (bcc) structure were also identified, indicating the presence of a small portion of Mo material in the sample. A typical scanning electron microscopy (SEM) image of the MoO_2 nanowires grown on the substrate is shown in Figure 1b. The image shows vertically aligned nanowires that are uniformly distributed over the entire substrate. The nanowires are straight, with diameters in the range of 50 to 120 nm and lengths of up to 4 μm.

The XRD pattern of the MoO_3 nanowire arrays is given in Figure 1c, and it reveals that the nanowires are highly crystalline. All of the diffraction peaks can be indexed to the orthorhombic structure MoO_3 with the lattice parameters: $a = 3.96$ Å, $b = 13.86$ Å, and $c = 3.7$ Å (JCPDS: 5-0508). A typical SEM image (Fig. 1d) shows that the nanowires have an analogous morphology to the MoO_2 nanowires, but with larger diameters.

A typical XRD pattern of the Mo nanowire arrays is shown in Figure 1e. This reveals that the Mo nanowires have a pure metallic bcc structure with lattice parameter $a = 3.14$ Å (JCPDS: 42-1120). The SEM image shown in Figure 1f illustrates that the nanowires retain their wire-like morphology but with smaller diameters: no distinct destruction was observed. Energy dispersive X-ray spectroscopy (EDX) was employed to analyze the elements in the Mo nanowires, and confirmed the absence of oxygen.

Further characterization of the nanowire arrays was performed by transmission electron microscopy (TEM). Figures 2a–c show typical TEM images of the MoO_2, MoO_3, and Mo nanowires, respectively, and these confirm that the nanowires are in the form of solid rods. A typical high-resolution TEM (HRTEM) image of the MoO_2 nanowires (Fig. 2d) along with the selected area electron diffraction (SAED) pattern (Fig. 2d, inset) show the internal structure of the MoO_2 nanowires. The two sets of parallel fringes with a spacing of 2.44 Å and 2.41 Å correspond to (200) and (002) planes, respectively. The same observation with the MoO_3 nanowire (Fig. 2e) provided further insight into the structure of the nanowires. The SAED pattern recorded perpendicular to the growth axis of a single nanowire could be attributed to the [010] zone axis diffraction of orthorhombic MoO_3. A typical HRTEM image of a Mo nanowire (Fig. 2f) shows lattice fringes with a spacing of 2.22 Å and the corresponding SAED pattern recorded perpendicular to the growth axis of the single nanowires could be attributed to the [001] zone axis diffraction of bcc Mo.

Based on the observations reported above, we propose a possible growth mechanism for the formation of the MoO_2 nanowire arrays. Since no catalyst was used in the original synthetic process, the growth of the MoO_2 nanowires may not be dominated by the vapor–liquid–solid (VLS) mechanism that is frequently employed to explain the growth of many nanowires.[17,18] A modified vapor–solid (VS) mechanism[19,20] may account for the observed nanostructures. In a typical VS process, the constituents of the nanowires are evaporated from a solid source in a high-temperature zone, and then directly deposited onto a substrate in a lower-temperature region. In our present work the only source is the Mo boat, and the main product is MoO_2 nanowire arrays. Also, we found that the growth process clearly involves oxygen, which may be residual in the chamber. We proposed the following growth model, illustrated in Figure 3, in the light of the existing VS mechanism. As the temperature gradually increased to, and at the final temperature of, 1100 °C, evaporation occurred at the surface of the Mo material in the boat under vacuum. The Mo vapor was transported to the vicinity of the substrate in the lower temperature region, where the Mo molecule may react with the remnant oxygen in the vacuum chamber. If the chamber was fed with a flow of oxygen, MoO_3 nanowires grew. On the other hand, if the vacuum chamber was fed with a flow of hydrogen, no nanowires grew. Considering the deficiency of oxygen in the chamber, unstable molybdenum oxide (MoO_x) may have formed. We suspect that, in the subsequent process,

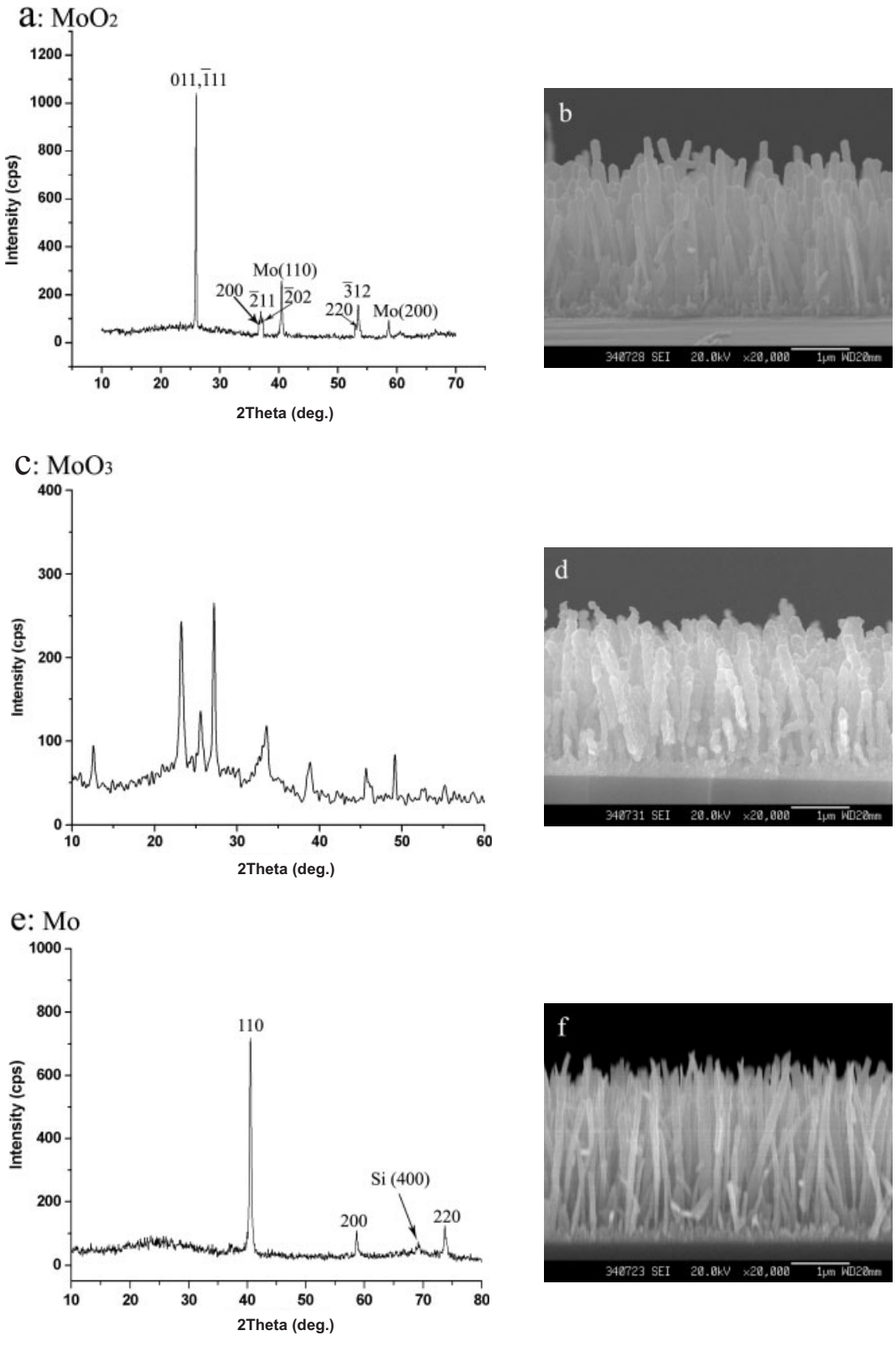

Fig. 1. a) The XRD spectrum of the MoO_2 nanowire arrays (monoclinic structure). b) A typical SEM image of the MoO_2 nanowire arrays grown on silicon substrates. c) A typical XRD spectrum of the MoO_3 nanowire ensembles, revealing the pure orthorhombic structure of MoO_3. d) A typical SEM image of the MoO_3 nanowire arrays on the silicon substrate. e) A typical XRD pattern of the Mo nanowire arrays (bcc structure). f) A typical SEM image of the Mo nanowire arrays, which shows their wire-like morphology.

ADVANCED MATERIALS

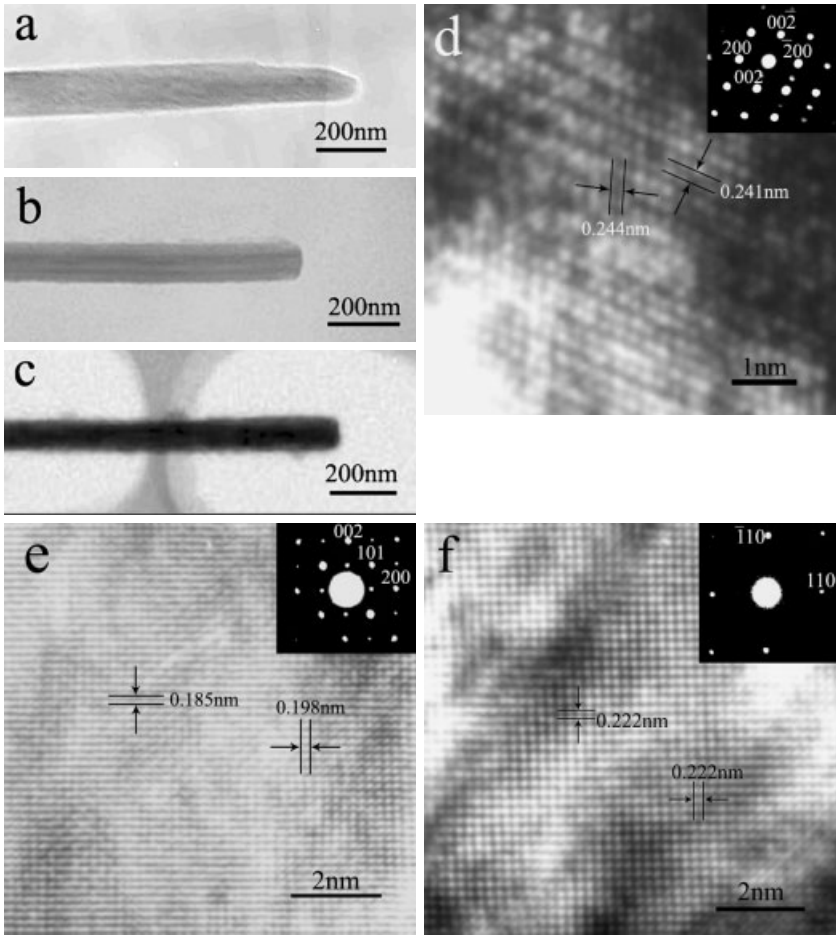

Fig. 2. a–c) Typical TEM images of MoO_2, MoO_3, and Mo nanowires, respectively. d–f) HRTEM images of the MoO_2, MoO_3, and Mo nanowires (and the corresponding SAED patterns), respectively.

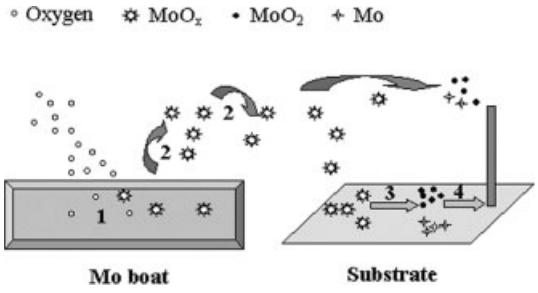

Fig. 3. The growth process proposed for the formation of MoO_2 nanowires (see text for details).

some MoO_x in the vapor phase condensed onto the substrate surface, forming unstable MoO_x in the solid phase. When this unstable solid MoO_x interacted with the vapor, it reacted with oxygen to become stable MoO_2. In the following process, MoO_x in the vapor phase may have combined with the MoO_2 seed to form nanowires. Very recently, we have applied this synthetic method to prepare tungsten and tungsten oxide nanowires.

As expected from the aligned nanowire structures, excellent field emission properties have been found. The field emission measurements were carried out in a vacuum chamber of $\sim 2.0 \times 10^{-7}$ torr at room temperature. The nanowire arrays were first adhered to the surface of an oxygen-free, high-conductivity copper disc using silver paint. A transparent anode, consisting of a quartz plate 4 cm in diameter and coated with conducting tin oxide film, was placed in front of, and parallel to, the surface of the sample cathode. Figure 4 shows typical plots of the field emission current versus the applied electric field of the metallic Mo, MoO_2, and MoO_3 nanowire arrays.

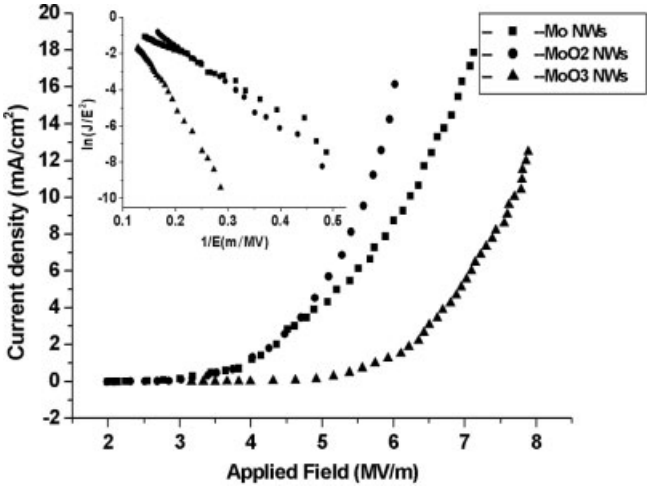

Fig. 4. Field emission current versus electric field (I–E) plots for the Mo (■), MoO_2 (●), and MoO_3 (▲) nanowire arrays and their corresponding FN plots (inset).

From the plots, we determined their field emission turn-on field (E_{to}) and threshold field (E_{thr}), which are defined to be the macroscopic fields required to produce a current density of 10 μA cm^{-2} and 10 mA cm^{-2}, respectively. As shown in Table 1, E_{thr} of the Mo, MoO_2, and MoO_3 nanowire arrays are 6.24 MV m^{-1}, 5.60 MV m^{-1}, and 7.65 MV m^{-1}, respectively.

Table 1. The emission turn-on fields and threshold fields (field required to generate a current density of 10 μA cm^{-2} and 10 mA cm^{-2}, respectively) for various emitter materials.

Material	Turn-on field [MV m^{-1}]	Threshold field [MV m^{-1}]
C nanotubes [21]	< 0.75	1.6
SiC nanowires [22]	0.9	~ 2.5–3.5
Cu_2S nanowires [23]	6.0	~ 12
MoO_3 nanobelts [24]	8.7	12.9
ZnO nanowires [25]	6.0	> 11
Mo nanowires	2.2	6.24
MoO_2 nanowires	2.4	5.6
MoO_3 nanowires	3.5	7.65

Although these values are higher than the best data from carbon nanotubes[21] and SiC nanowires,[22] they are much lower than those of many other nanomaterials, such as Cu_2S nanowires,[23] MoO_3 nanobelts,[24] and ZnO nanowires.[25] The fact that the field emission performance of the MoO_3 nanowires is much better than that of the MoO_3 nanobelts may be due to their better alignment. More importantly, nanowires of Mo oxides have a better field emission performance than metallic Mo nanowires. Therefore, it is not necessary to worry about the possibility of degrading these nanowire emitters during the process of making vacuum electronic and microelectronic devices, in which oxidation may occur in a number of ways.

The emission characteristics were analyzed using Fowler–Nordheim (FN) theory:[26]

$$J = (E^2\beta^2/\Phi)\exp(-B\Phi^{3/2}/E\beta) \quad (1)$$

where J is the emission current density, E is the applied field ($E = V/d$), Φ is the work function, β is the enhancement factor, and $B = 6.83 \times 10^9$ (eV$^{-3/2}$ V m^{-1}). By plotting $\ln(J/E^2)$ versus $1/E$, a straight line was obtained (see inset, Fig. 3). The linearity of these curves implies that the field emission from these nanowire arrays follows FN theory. By using the work function of bulk Mo (4.24 eV), β of our Mo nanowire arrays was calculated to be about 4400, which is high enough for various field emission applications.

In summary, nanowire arrays of Mo and its oxides were prepared on silicon substrates based on a process of thermal evaporation followed by further oxidation (for the oxide ensembles) or reduction (for the Mo ensembles). A growth mechanism for the MoO_2 nanowire arrays was proposed in the light of a special VS process. The method has promising applications for growing metallic, and corresponding oxide, nanowire arrays over a large area. In addition, the field emission properties of the prepared nanowire arrays were found to be better than those of many other nanomaterials. Thus, these nanomaterials have potential applications in vacuum microelectronic devices.

Experimental

Silicon (100) substrates (resistivity ~ 10 Ω cm; 10 mm × 5 mm) were first washed with hydrofluoric acid and then washed with alcohol in an ultrasonic cleaner. Then the substrates and the Mo boat (120 mm × 15 mm × 3 mm) were placed in the vacuum chamber (Φ 300 mm × 400 mm, Fig. 5). The substrates were separated from the boat with a spacing of 2 mm. The vacuum system was

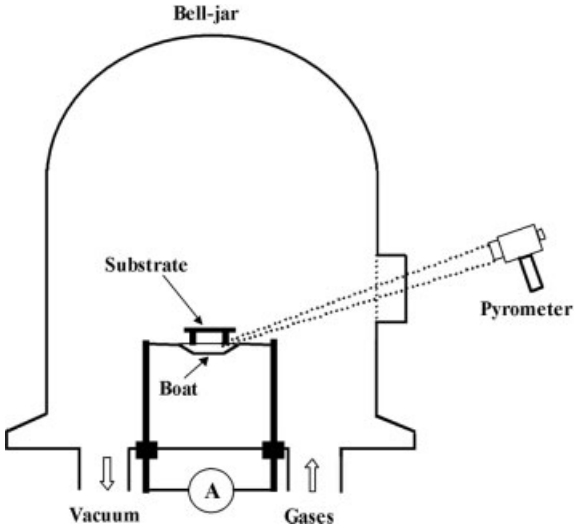

Fig. 5. Schematic diagram of the growth chamber and setup used to synthesize the nanowires.

first evacuated down to about 1.5×10^{-2} torr. Then high purity argon (99.99 %) was introduced to the chamber. The temperature of the Mo boat was then ramped to ~ 1100 °C at a rate of 100 °C min^{-1} and the boat was kept at that temperature for 60 min under a constant flow of argon gas (200 sccm, standard cubic centimeters per minute). Finally, the temperature was allowed to descend gradually to room temperature and MoO_2 nanowire arrays were produced on the substrates.

Further oxidation was carried out in the same vacuum chamber. The MoO_2 nanowire arrays were placed on the Mo boat, then the vacuum system was evacuated down to about 1.5×10^{-2} torr and high purity argon (99.99 %; 100 sccm) mixed with high purity oxygen (99.99 %; 100 sccm) was introduced into the chamber. The temperature of the boat was increased to about 400 °C at a rate of 100 °C min^{-1} and held there for 30 min. Finally, the temperature was allowed to descend gradually to room temperature.

The reduction in hydrogen was also carried out in the same vacuum chamber. The MoO_2 nanowire arrays were placed on the Mo boat, then the vacuum system was evacuated down to about 1.5×10^{-2} torr and a constant flow (200 sccm) of high-purity H_2 (99.99 %) was introduced to the chamber; the temperature of the boat was increased to 800 °C at a rate of 100 °C min^{-1} and held there for 10 h. Finally, the temperature was allowed to descend gradually to room temperature.

The nanowire arrays were analyzed by XRD (D/max-3A apparatus), Raman spectroscopy (LABRAM-1B apparatus, $\lambda = 632.81$ nm), SEM (JSM-6330F operated at 20 kV), TEM (JEM-2010 operated at 200 kV), TEM (Phillips EM200 operated at 160 kV), and EDX (installed in Phillips EM200).

The field emission studies were carried out in a chamber having a vacuum of ~ 2.0×10^{-7} torr at room temperature. The sample areas were all about 2 mm^2 and in disc form, and they were first adhered to the surface of an oxygen-free, high-conductivity copper disc using silver paint. A manipulator (Huntington PM-600-T apparatus) was used to control the separation (d) between the anode and the cathode. The same vacuum gap (i.e., 0.30 mm) was used when the field emission properties of the Mo, MoO_2, and MoO_3 nanowire arrays were measured. A charge coupled device (CCD) camera was used to record the spatial distribution of the emission sites.

Received: June 13, 2003
Final version: July 22, 2003

ADVANCED MATERIALS

[1] M. H. Huang, S. Mao, H. Feick, H. Q. Yan, Y. Y. Wu, H. Kind, E. Weber, R. Russo, P. D. Yang, *Science* **2001**, *292*, 1897.
[2] A. Kolmakov, Y. X. Zhang, G. S. Cheng, M. Moskovits, *Adv. Mater.* **2003**, *15*, 997.
[3] C. R. Martin, *Science* **1994**, *266*, 1961.
[4] H. Cao, Z. Xu, H. Sang, D. Deng, C. Tie, *Adv. Mater.* **2001**, *13*, 121.
[5] M. J. Edmondson, W. Zhou, S. A. Aiber, I. P. Jones, I. Gameson, P. A. Anderson, P. P. Edwards, *Adv. Mater.* **2001**, *13*, 1608.
[6] J. Murphy, N. R. Jana, *Adv. Mater.* **2002**, *14*, 80.
[7] A. J. Yin, J. Li, W. Jian, A. J. Bennett, J. M. Xu, *Appl. Phys. Lett.* **2001**, *79*, 1039.
[8] I. V. Malikov, G. M. Mikhailov, *J. Appl. Phys.* **1997**, *82*, 5555.
[9] S.-L. Zhang, F. M. d'Heurle, *Appl. Phys. Lett.* **2000**, *76*, 1831.
[10] Y. K. Liu, C. G. Liang, Z. L. Wang, Y. Z. He, X. L. Lan, M. H. Zhou, *Jpn. J. Appl. Phys., Part 1* **2000**, *39*, 3915.
[11] Y. Liu, Y. Qian, M. Zhang, Z. Chen, C. Wang, *Mater. Res. Bull.* **1996**, *31*, 1029.
[12] Z. Hussain, *J. Mater. Res.* **2001**, *16*, 2695.
[13] H. C. Zeng, *Inorg. Chem.* **1998**, *37*, 1967.
[14] J. N. Yao, K. Hashimoto, A. Fujishima, *Nature* **1992**, *355*, 624.
[15] M. P. Zach, K. H. Ng, R. M. Penner, *Science* **2000**, *290*, 2120.
[16] X. L. Li, J. F. Liu, Y. D. Li, *Appl. Phys. Lett.* **2002**, *81*, 4832.
[17] X. F. Duan, C. M. Lieber, *Adv. Mater.* **2000**, *12*, 298.
[18] M. H. Huang, Y. Y. Wu, H. N. Feick, N. Tran, E. Weber, P. D. Yang, *Adv. Mater.* **2001**, *13*, 113.
[19] Z. W. Pan, Z. R. Dai, Z. L. Wang, *Science* **2001**, *291*, 1947.
[20] Z. R. Dai, Z. W. Pan, Z. L. Wang, *Adv. Funct. Mater.* **2003**, *13*, 9.
[21] A. M. Rao, D. Jacques, R. C. Haddon, W. Zhu, C. Bower, S. Jin, *Appl. Phys. Lett.* **2000**, *76*, 3813.
[22] Z. W. Pan, H. L. Lai, F. C. K. Au, X. F. Duan, W. Y. Zhou, W. S. Shi, N. Wang, C. S. Lee, N. B. Wong, S. T. Lee, S. S. Xie, *Adv. Mater.* **2000**, *12*, 1186.
[23] J. Chen, S. Z. Deng, N. S. Xu. S. H. Wang, X. G. Wen, S. H. Yang, C. L. Yang, J. N. Wang, W. K. Ge, *Appl. Phys. Lett.* **2002**, *80*, 3620.
[24] Y. B. Li, Y. Bando, D. Golberg, K. Kurashima, *Appl. Phys. Lett.* **2002**, *81*, 5048.
[25] C. J. Lee, T. J. Lee, S. C. Lyu, Y. Zhang, H. Ruh, H. J. Lee, *Appl. Phys. Lett.* **2002**, *81*, 3648.
[26] R. H. Fowler, L. W. Nordheim, *Proc. R. Soc. London, Ser. A* **1928**, *119*, 173.

Unique Single-Crystalline Beta Carbon Nitride Nanorods**

By *Long-Wei Yin*,* *Yoshi Bando*, *Mu-Sen Li*, *Yu-Xian Liu*, and *Yong-Xin Qi*

The discovery of the carbon nanotube has opened a challenging new field in materials, solid-state physics, and chemistry, offering a wide perspective for many possible applications.[1] The successful synthesis of functional ceramic micro- or nanostructures such as BN,[2,3] WS_2,[4] MoS_2,[5] In_2O_3,[6] TiO_2,[7] and so forth has been reported. The theoretical prediction of a super-hard carbon nitride solid of composition C_3N_4 (space group $P6_3/m$) by Liu and Cohen[8] has directed the efforts of many experimental groups to synthesize this compound.[9–14] It has been extensively claimed that the carbon nitride compound could be formed in thin amorphous films by several methods such as shock-wave compression technology, pyrolysis of high nitrogen content precursors, diode sputtering, solvothermal preparation, pulsed laser ablation, and ion implantation. The hypothetical β-C_3N_4 has the same crystal structure as β-Si_3N_4, with a hexagonal network of tetrahedrally (sp^3) bonded carbon and trigonal planar nitrogen (sp^2). Besides its predicted hardness, carbon nitride is also considered to be very promising in the fields of tribological and wear-resistance coating and optical and electronic engineering.[15–19]

Although extensive studies on the synthesis and the characterization of carbon nitride materials have been reported, so far the nitrogen concentration of the formed carbon nitrogen compound is usually below the ideal composition for C_3N_4. Furthermore, the bonding between C and N tends to be of sp^2-type character. An appropriate synthetic route to obtain the C_3N_4 solid is still unknown. The difficulties in the synthesis of hard carbon nitrides are very likely related to their low thermodynamic stability with respect to the elements (C and N), indicated by a positive value of the enthalpies of formation.[20] Therefore, it will be particularly important to find effective and low-cost methods for synthesizing carbon nitride single crystals with a chemical composition of 3:4 for C/N.

With this aim in view, we have recently succeeded for the first time in synthesizing single crystal β-C_3N_4 nanorods in gram quantities via a simple route. As is known, the mechanochemical reaction may offer a possible method for materials synthesis under non-equilibrium condition with several advantages over conventional methods such as the production of non-aggregate and uniform particles in the nanometer scale range.[21,22] It may be used to drive a wide range of chemical reactions and can be performed under a controlled atmosphere to initiate solid–solid and solid–gas reactions to obtain special phases that could only be synthesized under extreme conditions such as high pressure and high temperature (HPHT), thus providing a low-cost method for synthesizing carbon nitride crystal. In this communication, nanostructured porous amorphous carbon powders with a high surface area and structural defects were firstly obtained by a high-energy mechanical process, then they were continually high-energy ball milled under a NH_3 atmosphere. Afterwards the formed carbon nitride compounds were thermally annealed in NH_3 gas flow at different temperatures. It was found that the β-C_3N_4 uniform single crystal nanorods were formed during the subsequent thermal annealing. Combined material characterization data from X-ray diffraction (XRD), high-resolution transmission electron microscopy (HRTEM), X-ray photoelectron spectroscopy (XPS), electron energy loss spectroscopy (EELS), and Fourier transform infrared spectroscopy (FTIR) provide substantial evidence for the formation of the β-C_3N_4 structure. This communication reports an effective, low-cost, and high-yield method for the synthesis of single crystal β-C_3N_4 nanorods.

[*] Dr. L.-W. Yin, Prof. Y. Bando
Advanced Materials Laboratory
National Institute for Materials Science
Namiki 1–1, Tsukuba, Ibaraki 305–0044 (Japan)
E-mail: Yin.Longwei@nims.go.jp
Dr. L.-W. Yin, Prof. M.-S. Li, Y.-X. Liu, Dr. Y.-X. Qi
College of Materials Science and Engineering
Shandong University
73 Jing Shi Road, Jinan 250061 (P. R. China)

[**] This work was supported by Doctor Science Foundation of Chinese Education Ministry [Project No. 20020422035].

  DOI: 10.1002/adma.200305307